January 2010

Lattice thermal conductivity of freestanding gallium nitride nanowires

Jie Zou
Eastern Illinois University, jzou@eiu.edu

Lattice thermal conductivity of freestanding gallium nitride nanowires

Jie Zou[a)]

Department of Physics, Eastern Illinois University, Charleston, Illinois 61920, USA

We report detailed calculations of the lattice thermal conductivity of freestanding gallium nitride (GaN) nanowires with diameters ranging from 20 to 140 nm. Results are compared with experimental data on GaN nanowires grown by thermal chemical vapor deposition (CVD). Calculations are based on the Boltzmann transport equation and take into account the change in the nonequilibrium phonon distribution in the case of diffuse scattering at the surfaces. Phonon dispersion relation is obtained in the elastic continuum approximation for each given nanowire. For valid comparisons with the experimental data, simulations are performed with a dopant concentration and impurity profile characteristic of thermal CVD GaN nanowires. Our results show that the room-temperature thermal conductivity of the nanowires has very low values, ranging from 6.74 W/m K at 20 nm to 16.4 W/m K at 140 nm. The obtained results are in excellent agreement with the experimental data. We have also demonstrated that in addition to impurity scattering, boundary scattering, and phonon confinement, the change in the nonequilibrium phonon distribution leads to a further reduction in the thermal conductivity of the nanowires and has to be taken into account in the calculations. Our conclusion is different from that of an earlier study which attributed the very low thermal conductivity to the unusually large mass-difference scattering in the nanowires. © *2010 American Institute of Physics.* [doi:10.1063/1.3463358]

I. INTRODUCTION

GaN nanowires have attracted significant attention due to their applications in high-power/high-temperature photonic, optoelectronic, and electronic devices, including GaN-based quantum wire UV lasers and high electron mobility transistors.[1,2] Quasi-one-dimensional nanostructures, such as GaN nanowires, have been proposed as the building blocks for future nanoscale photonic devices.[3,4] One example is the multicolor, high-efficiency, light-emitting diodes based on GaN core/mutishells nanowire heterostructures.[3] The possibility of integrating nanowire-based photonic devices with conventional silicon microelectronics has also been demonstrated.[4]

The envisioned high-power/high-temperature device applications based on GaN nanowires require accurate knowledge of the thermal conductivity of these materials. So far, most of the theoretical and experimental work has focused on the thermal conductivity of bulk GaN and micrometer-thick GaN films.[5–8] There have been very few reports on the thermal conductivity of GaN nanowires.[9,10] One of the reports[9] involved the molecular dynamics (MD) simulation of the size and orientation dependence of the thermal conductivity of GaN nanowires, but only for very small diameters in the range of 2.02–6.44 nm. Thus, even though MD simulation can provide an accurate result of thermal conductivity by directly simulating atomic motions, it is mainly applied to wires of very small diameters due to limitation in the computational power. More recently, using a suspended island method, Guthy *et al.*[10] measured the thermal conductivity of individual freestanding GaN nanowires grown by thermal chemical vapor deposition (CVD) with diameters in the

range of 97–181 nm. They observed "unexpectedly" low thermal conductivity of the nanowires, ranging from 13 to 19 W/m K at room temperature, and weak diameter dependence. As a comparison, the thermal conductivity of an ideal bulk GaN crystal at room temperature was predicted to be as high as 410 W/m K by Witek.[5] Liu *et al.*[7] measured the thermal conductivity of thick (~ 100 μm) GaN films grown by hydride vapor phase epitaxy (HVPE) and found that for the best sample (dislocation density $\sim 10^6$ cm^{-2} and dopant concentration $\sim 10^{16}$ cm^{-3}) the room-temperature thermal conductivity was 225 W/m K. To explain the very low thermal conductivity observed in the GaN nanowires, Guthy and co-workers performed detailed simulations. Based on the simulation results, they concluded that the "unexpectedly" low thermal conductivity was due to the "unusually" large mass-difference scattering in the samples. However, it is important to note that in their simulations several fitting parameters were used, including the impurity concentrations, the phonon group velocity, and the phonon mean free path, L_C, due to boundary scattering. In order to obtain a good fit to the experimental data, they assumed unusually high values for the Si and O impurity concentrations, both reaching the upper limit of their respective concentration range as determined by the electron-energy-loss spectroscopy (EELS) measurement. In addition, to reach a best fit, L_C was set much smaller than the corresponding wire diameter. The very small values for L_C were attributed to the stacking faults present in the samples.

In this paper, we present detailed modeling and simulation of the thermal conductivity of GaN nanowires for a wide range of diameters. Our model is based on the Boltzmann transport equation (BTE) approach, but explicitly takes into account the change in the nonequilibrium phonon distribu-

a)Electronic mail: jzou@eiu.edu.

034324-2   Jie Zou

tion in the case of diffuse scattering at the wire surfaces—a factor that was not considered in the previous study in Ref. 10. Moreover, in our simulations we do not use fitting parameters, but rather obtain the phonon dispersion (and group velocity) for each given nanowire and calculate thermal conductivity using a characteristic dopant concentration and impurity profile determined by the experiments. The effects of impurity scattering, boundary scattering, phonon confinement, and the change in the nonequilibrium phonon distribution due to diffuse surface scattering are also discussed. Finally, we compare our results with the experimental data reported in Ref. 10.

The rest of the paper is organized as follows. In Sec. II, we present details of the theoretical model. Simulation results are discussed in Sec. III. Conclusions are presented in Sec. IV.

II. THEORY AND MODEL

A. Phonon BTE and thermal conductivity

We calculate the lattice thermal conductivity, κ, based on the BTE approach. In this approach, thermal conductivity is derived based on the solution of the steady-state phonon BTE in the presence of a temperature gradient. The solution deviates from the value in equilibrium and represents the nonequilibrium phonon distribution, from which the thermal conductivity can be derived. In general, there are two different methods to solve the BTE: the variational and the relaxation-time methods.[11] The former applies the variational principle to obtain the solution, while the latter assumes a well-defined total relaxation time for the various phonon scattering processes. Derivation for the thermal conductivity of bulk semiconductors based on the solution of the BTE in the relaxation-time approximation has been discussed in detail, for example, by Bhandari and Rowe.[11] Assuming a small temperature gradient, the thermal conductivity in the bulk, κ_{bulk}, can be expressed as[11]

$$\kappa_{\text{bulk}} = \left(\frac{k_B}{\hbar}\right)^3 \frac{k_B}{2\pi^2 V} T^3 \int_0^{\theta_D/T} \frac{\tau_C x^4 e^x}{(e^x - 1)^2} dx, \qquad (1)$$

where k_B and $\hbar$ are the Boltzmann and Planck constants, V is the sound velocity, T is the absolute temperature, θ_D is the Debye temperature, τ_C is the combined (total) relaxation time due to phonon scattering, and $x \equiv \hbar\omega/k_B T$ with ω being the phonon angular frequency. Equation (1) is also known as the Klemens–Callaway's expression for the thermal conductivity in the bulk. Balandin and Wang[12] have applied this equation to the calculation of κ of nanoscale thin films by including modification of the phonon dispersion and group velocity, V, due to phonon confinement. This approach has also been applied to the calculation of κ of nanowires.[13] Later, Walkauskas et al.[14] corrected Eq. (1) for a nanowire by taking into account the deviation of the nonequilibrium phonon distribution from its bulk value due to diffuse boundary scattering at the wire surface. However, their original formulation did not include the effect of phonon confinement, but instead used the phonon dispersion in the bulk. Subsequently, Zou and Balandin[15] combined the above two approaches in the calculation of the thermal conductivity of Si nanowires,

but only for a specific wire diameter of 20 nm.

In the present work, we follow the combined approach and perform detailed calculations of the thermal conductivity of GaN nanowires with diameters ranging from 20 to 140 nm, and compare our results with recent experimental data. In the combined approach, the thermal conductivity of a nanowire is given by[14,15]

$$\kappa_{\text{wire}} = \left(\frac{k_B}{\hbar}\right)^3 \frac{k_B}{2\pi^2 \bar{V}} T^3 \int_0^{\theta_D/T} \frac{\tau_C(x) x^4 e^x}{(e^x - 1)^2}$$
$$\times \left\{ 1 - \frac{24}{\pi} G[p(x)] \right\} dx. \qquad (2)$$

Detailed derivation of the above equation has been discussed in Refs. 14 and 15. Equation (2) is derived for a nanowire of a cylindrical geometry. In this equation, $\bar{V}$ is the overall phonon group velocity calculated for a given nanowire. To obtain $\bar{V}$, the frequency-dependent phonon group velocity, $V_n(\omega)$, for each phonon dispersion branch, n, is first calculated; $\bar{V}$ is then found by averaging $V_n(\omega)$ over the phonon branches and phonon frequencies. Calculations for the phonon dispersion and group velocity are discussed in Sec. II B and those for the combined relaxation time are discussed in Sec. II C. The second term in Eq. (2) in the curly brackets arises from the correction to the bulk formula due to the change in the nonequilibrium phonon distribution in the case of diffuse boundary scattering at the wire surface. The parameter p is defined as the ratio between the wire diameter, D, and the phonon mean free path, L, i.e., $p(x) = D/L(x)$, where $L(x) = \bar{V} \cdot \tau_C(x)$. In the case of purely diffuse boundary scattering, function G is defined as[14]

$$G(p) = \int_0^1 (1 - y^2)^{1/2} S_4(py) dy, \qquad (3)$$

where

$$S_4(u) = \int_0^{\pi/2} \exp(-u/\sin\theta) \cos^2\theta \sin\theta d\theta. \qquad (4)$$

In a general case of partially specular and partially diffuse boundary scattering, function G is given by a more complex form[14] and depends on the specularity parameter, ε, which is defined as the fraction of the phonons that are scattered specularly at the surface. The value of ε is between 0 and 1, with $\varepsilon = 0$ representing a purely rough surface and $\varepsilon = 1$ representing a purely smooth surface. In the previous work,[15] ε has been treated as a simulation parameter, but in practice it depends on the phonon wavelength, λ, and the asperity parameter, η, of the surface. The latter represents the mean variation in the surface and is defined as the root-mean-square deviation of the height of the surface from the reference plane.[16] According to Ziman,[16] ε is related to λ and η by $\varepsilon(\lambda) = \exp(-16\pi^3\eta^2/\lambda^2)$. At room temperature, most of the heat in nonmetallic solids is carried by phonons with wavelengths of a few nanometers.[17] For these phonons, even a very small asperity value of a few angstroms can result in an almost perfectly rough surface at which purely diffuse scattering occurs (i.e., $\varepsilon = 0$). For example, $\varepsilon = 0.007$ when

$\lambda = 3$ nm and $\eta = 3$ Å. Thus, in this paper we focus on the case of purely diffuse boundary scattering when calculating thermal conductivity. A more general formulation can be found in Refs. 14 and 15.

B. Confined phonon dispersion relation and group velocity

Acoustic waves in cylindrical rods were first studied in the context of waveguides, where dispersion relations were obtained by various methods, including the potential theory, the superposition of partial waves, and the transverse resonance method.[18] It is known that in a free-surface cylindrical rod, the longitudinal acoustic (LA) waves propagate along the axis of the rod while the waves are coupled modes of axial and radial motions. These waves are also called the dilatational modes since the radial component of the vibration causes the surface of the rod to dilate and contract. More recently, dispersion relations of confined acoustic phonon modes in cylindrical nanowires were derived based on the elastic continuum approximation.[19] In this approach, one starts with the elastic wave equation of a given medium and look for solutions in the form of traveling waves. Appropriate boundary conditions, free-surface or clamped-surface, are then applied to the above solutions and phonon dispersions can be obtained. Here, we focus on the case of free-surface nanowires since the thermal conductivity of freestanding GaN nanowires[10] has been measured recently. Also, in the present work we consider LA phonon modes. It has been shown that these modes dominate thermal conduction at room temperature.[17] For a free-surface cylindrical nanowire, phonon dispersions for the LA modes can be calculated from the following equation:[19]

$$(k^2 - k_t^2)^2 \frac{(k_l a)J_0(k_l a)}{J_1(k_l a)} - 2k_l^2(k^2 + k_t^2) + 4k^2 k_l^2 \frac{(k_t a)J_0(k_t a)}{J_1(k_t a)}$$
$$= 0, \qquad (5)$$

where k is the component of the wave vector along the wire axis (i.e., the propagation direction), k_t and k_l are the transverse wave vector components of the radial and axial motions, respectively, a is the radius of the wire, and J_0 and J_1 are the ordinary Bessel functions. The two parameters, k_t and k_l, in Eq. (5) are further related to the propagation wave vector k and angular frequency ω by

$$k_{l,t}^2 = \frac{\omega^2}{V_{l,t}^2} - k^2, \qquad (6)$$

where V_l and V_t are the longitudinal and transverse sound velocities in the bulk.

The above equations for the phonon dispersion relations are derived for an isotropic cylindrical nanowire. In an isotropic medium, solutions of the acoustic waves are independent of the direction of propagation and consist of a pure longitudinal (L) and two pure, degenerate transverse (T) modes. Sound velocities for the L and T modes are given by $V_l = (C_{11}/\rho)^{1/2}$ and $V_t = (C_{44}/\rho)^{1/2}$, respectively, where ρ is the mass density and C_{11} and C_{44} are elastic stiffness constants. In an anisotropic crystal, such as wurtzite GaN, wave solutions depend on the particular direction of propagation. The

solution for the phonon dispersion in an arbitrary direction is generally much more complex than that in the isotropic case. An alternative approach is to apply the isotropic assumption to certain propagation directions, along which the waves are reduced to pure L and T modes.[19] This approach has been used for the calculation of phonon dispersion in GaAs nanowires of cubic symmetry.[19] Here, we follow the spirit of this approach and consider a wurtzite GaN nanowire with the wire axis along the [001] direction (i.e., the c axis) of the GaN crystal. In this direction, the acoustic waves are given by a pure L mode and two pure, degenerate T modes with $V_l = (C_{33}/\rho)^{1/2}$ and $V_t = (C_{44}/\rho)^{1/2}$.[20]

To obtain the phonon dispersion relation in a nanowire, we first substitute Eq. (6) in Eq. (5), which is then reduced to an equation of the form $f(k,\omega) = 0$. Phonon dispersion relation, $\omega(k)$, can be found numerically by solving for ω at each given value of k. Phonon group velocity, $V_n(\omega)$, for each dispersion branch can then be calculated by numerical differentiation, i.e., $V_n = d\omega_n/dk$. We next obtain a branch-averaged, frequency-dependent phonon group velocity, $V(\omega)$. Different averaging methods have been proposed previously, including one that is based on the Callaway's formulation for a single polarization-averaged phonon branch[21] and one that involves the use of a Boltzmann factor.[13] Here, we use an alternative method and define the branch-averaged phonon group velocity, $V(\omega)$, as follows: at a given frequency ω, the dominant phonon branch is defined as the one that has the largest group velocity; the velocity of the dominant branch is then assigned to $V(\omega)$. The overall phonon group velocity, $\bar{V}$, is found by averaging $V(\omega)$ over phonon frequencies and is then used in Eq. (2) in the calculation of κ_{wire}.

C. Phonon scattering and relaxation times

It has been shown that in contrast to bulk GaN films, which typically suffer from high densities of threading dislocations, GaN nanowires can be grown almost dislocation-free.[22] Thus, in this work we do not include phonon scattering on dislocations. However, studies[22] on vapor-liquid-solid-grown GaN nanowires have revealed that the nanowires are n-doped with a dopant concentration of $\sim 2 \times 10^{19}$ cm^{-3}. The EELS measurements have also shown that the Si and O impurity concentrations are in the range of $0.1-1$ at. % and $0.01-0.1$ at. %, respectively. Therefore, in our model we consider the following phonon scattering processes: three-phonon Umklapp scattering (τ_U) due to the anharmonicity of the crystal, point-defect scattering (τ_P) due to impurities, phonon–electron scattering (τ_{Ph-e}), and boundary scattering (τ_B). The total (combined) relaxation time, τ_C, is found through $1/\tau_C = 1/\tau_U + 1/\tau_P + 1/\tau_{Ph-e} + 1/\tau_B$.

According to Klemens' second-order perturbation theory, the scattering rate for three-phonon Umklapp scattering at room temperature ($T = 300$ K) and above is given by[23]

$$\frac{1}{\tau_U} = 2\gamma^2 \frac{k_B T}{\mu V_0} \frac{\omega^2}{\omega_D}, \qquad (7)$$

where γ is the Gruneisen anharmonicity parameter, $\mu = V_t^2 \rho$ is the shear modulus, V_0 is the volume per atom of the crystal, and $\omega_D = k_B \theta_D/\hbar$ is the Debye frequency. For wurtzite

GaN, $V_0 = 3^{1/2}a^2c/8$, where a and c are the lattice constants. The material parameters are $\gamma = 0.74$,[5] $\mu = 105$ GPa, $V_0 = 11.42$ Å[3], and $\theta_D = 830$ K.[5] The values for μ and V_0 are based on $C_{44} = 105$ GPa, $a = 3.189$ Å, and $c = 5.185$ Å given by Ref. 20. Phonon scattering on point defects can be written as[24]

$$\frac{1}{\tau_P} = \frac{V_0 \Gamma \omega^4}{4\pi V^3},$$ (8)

where Γ is a quantity measuring the strength of the point-defect scattering and V is the phonon group velocity. In our model, V is given by the overall phonon group velocity, $\bar{V}$. In calculating Γ, we follow Klemens' original formulation[25] and consider scattering due to both mass and strain-field fluctuations. The former is caused by the difference in mass between the impurity and host atoms, whereas the latter is produced by the difference in size and coupling forces. Yang *et al.*[26] have recently reported the effects of strain-field fluctuations on the thermal conductivity of ZrNiSn-based thermoelectric compounds. The strength of the point-defect scattering is then given by[11,25]

$$\Gamma = \sum_i f_i \left[\left(1 - \frac{M_i}{\bar{M}}\right)^2 + 2\left\{6.4\gamma\left(1 - \frac{R_i}{\bar{R}}\right)\right\}^2 \right],$$ (9)

where f_i is the fractional concentration of the impurity atoms, M_i is the mass of the ith impurity atom, $\bar{M}$ is the average atomic mass, R_i is the Pauling ionic radius of the ith impurity atom, and $\bar{R}$ is the average radius. Here, we use an impurity concentration of 0.13 at. % for Si and 0.01 at. % for O. Note that these values are within the experimentally determined range for Si and O impurity levels.[22] The calculated value for Γ is 2.49×10^{-2}, which is similar in order of magnitude to that reported in Ref. 10. However, it should be pointed out here that in evaluating Γ, we have taken into account both the mass (Γ_M) and strain-field (Γ_S) fluctuations in the lattice. Our calculations show that $\Gamma_M = 1.789 \times 10^{-4}$ and $\Gamma_S = 2.47 \times 10^{-2}$, suggesting a much stronger contribution from the strain-field fluctuation than that from the difference in mass. Note that in Ref. 10 only mass-difference scattering was considered, which led to unusually large estimations for the impurity concentrations. Boundary scattering contributes to thermal resistance in the case of purely or partially diffuse scattering at the surfaces.[16] As discussed previously, the roughness of a surface can be characterized by a specularity parameter, ε. For a cylindrical wire, the boundary scattering rate is given by the following expression according to Ziman:[16]

$$\frac{1}{\tau_B} = \frac{V}{D}\left[\frac{1 - \varepsilon(\lambda)}{1 + \varepsilon(\lambda)}\right],$$ (10)

where D is the diameter of the wire and V is the phonon group velocity. As shown in Sec. II A, at room temperature, even a very small mean surface variation can result in diffuse scattering. Thus, here we consider the case of purely diffuse scattering of phonons at the wire surfaces such that $\varepsilon \to 0$. In this case, Eq. (10) is reduced to $1/\tau_B = V/D$, which we use in our simulations. We also replace V with the overall phonon
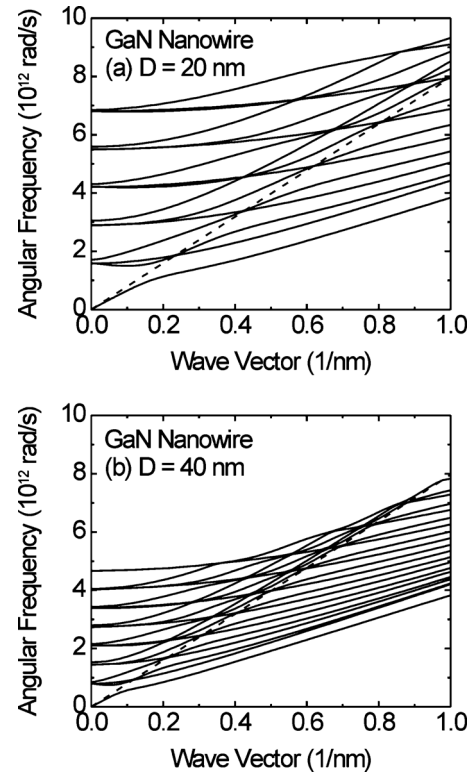

FIG. 1. Dispersion relations for LA phonon modes of freestanding GaN nanowires with diameters of (a) $D = 20$ nm and (b) $D = 40$ nm. Several lowest phonon branches are shown. The dashed lines indicate the dispersion relation for LA phonon modes in bulk GaN.

velocity, $\bar{V}$, calculated for a given nanowire. In a general case, where boundary scattering is partially diffuse and partially specular (i.e., $0 < \varepsilon < 1$), $1/\tau_B < V/D$. Finally, acoustic phonon scattering on electrons can be expressed as[27]

$$\frac{1}{\tau_{ph-e}} = \frac{n_e E_1^2 \omega}{\rho V^2 k_B T} \sqrt{\frac{\pi m^* V^2}{2 k_B T}} \exp\left(-\frac{m^* V^2}{2 k_B T}\right),$$ (11)

where n_e is the concentration of conduction electrons, E_1 is the deformation potential, ρ is the mass density, and m^* is the electron effective mass. In Eq. (11), $n_e = 2.3 \times 10^{19}$ cm^{-3}, which is characteristic of GaN nanowires grown by thermal CVD.[10,22] Other parameters include $\rho = 6150$ kg/m^3, $E_1 = 10.1$ eV, and $m^* = 0.22 m_e$, where m_e is the electron mass.[10] An alternative expression for $1/\tau_{Ph-e}$ was obtained by Ziman using the effective mass approximation and can be found in Refs. 10 and 27.

III. SIMULATION RESULTS AND DISCUSSIONS

First, phonon dispersion relations are calculated for LA phonon modes in freestanding GaN nanowires with various diameters, ranging from 20 to 140 nm with an increment of 20 nm. The bisection numerical method is applied to solve Eqs. (5) and (6) for phonon angular frequency, ω, at each given value of the phonon wave vector, k. Results for $D = 20$ and 40 nm are shown in Figs. 1(a) and 1(b), respectively. The dashed line in each figure indicates the dispersion relation in bulk GaN for LA phonon modes. It can be seen in both (a) and (b) that the dispersion relation of a nanowire consists of discrete phonon branches. This feature is com-
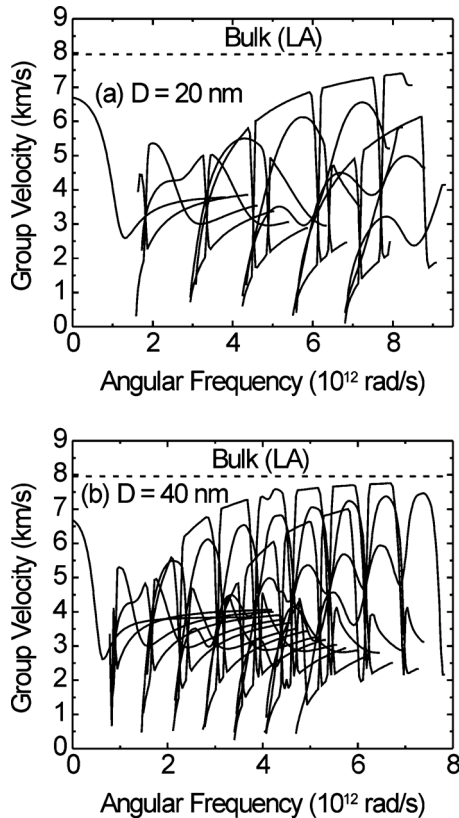
FIG. 2. Phonon group velocity as a function of phonon angular frequency calculated for each dispersion branch. The results are shown for (a) D =20 nm and (b) D=40 nm. The dashed lines indicate the sound velocity for LA phonon modes in bulk GaN.

FIG. 3. Branch-averaged phonon group velocity as a function of phonon angular frequency for D=20 and 40 nm. The horizontal dashed-dotted line indicates the sound velocity in bulk GaN for LA phonon modes. The results for D=20 nm are obtained in two methods: using the isotropic assumption (solid curve) and assuming phonon propagation in the [001] direction of wurtzite GaN (dashed curve).

mon for dispersion relations in nanostructures, and has been observed in nanoscale thin films,[12] nanowires,[19] and heterostructures.[21] The physical origin for the discrete phonon branches is the quantization of the wave vector component in the confined direction due to boundary conditions at the surfaces. In a nanowire, k_l and k_t in Eq. (6) are quantized. Thus, for each given value of k there exists discrete values of ω, resulting in discrete phonon branches. It can also be seen in both (a) and (b) that the slope of each phonon branch is less than that of the bulk dispersion, indicating a decreased phonon group velocity in a nanowire compared to that in the bulk. The modification of the phonon dispersion and group velocity in a nanostructure is referred to as the phonon confinement effect.[12] When comparing (a) and (b), one can also see that with an increase in the wire diameter, the initial values for ω at k=0 become lower and the phonon branches become more closely spaced from each other. This indicates that phonon confinement becomes less prominent with increasing diameter of the nanowire. In the limiting case where the lateral dimension of a nanostructure, e.g., the thickness of a thin film, approaches infinity, quantization of the wave vector component in the confined direction will become insignificant and the phonon branches will become infinitely close together and approach that of the bulk dispersion.

Phonon group velocity as a function of phonon angular frequency is shown for individual branches in Figs. 2(a) and 2(b). The dashed line in each figure indicates the longitudinal sound velocity in bulk GaN. It can be seen that in a free-
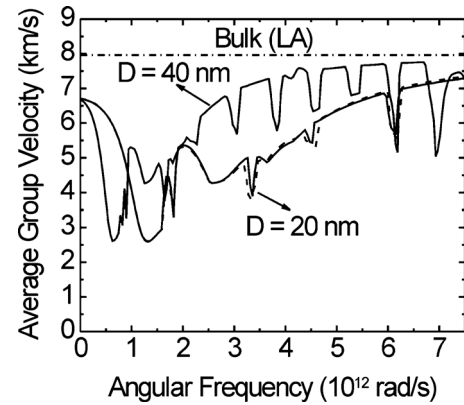
standing nanowire, the phonon group velocities are lower than the corresponding bulk sound velocity for all phonon branches. It is important to point out that the above results are calculated under the free-surface boundary condition. Balandin and co-workers[28] have reported calculations of phonon dispersion in coated cylindrical nanowires, where the interface between the nanowire and its coating material represents an intermediate boundary condition. Their results show that in contrast to a freestanding nanowire, phonon group velocity in the active layer of a coated nanowire can be made higher or lower than the corresponding bulk velocity by appropriately selecting the barrier material and barrier thickness, thus suggesting the possibility of engineering thermal transport properties in nanostructures. Next, we obtain the branch-averaged phonon group velocity as a function of phonon frequency. Results for D=20 and 40 nm are both shown in Fig. 3. It can be seen that overall, phonon group velocity increases with increasing wire diameter. This result is expected since in the limiting case of $D \rightarrow \infty$, phonon group velocity should approach that in the bulk for all frequencies. Also, to investigate the effects of the anisotropy of wurtzite GaN, we calculate the dispersion relation and group velocity for the case of D=20 nm using two sets of parameters: in set I, we follow the isotropic assumption and use $V_l=(C_{11}/\rho)^{1/2}$ and $V_t=(C_{44}/\rho)^{1/2}$; in set II, we assume that phonon propagation is along the [001] direction and use V_l $=(C_{33}/\rho)^{1/2}$ and $V_t=(C_{44}/\rho)^{1/2}$. The elastic stiffness constants are taken from Ref. 20 and given by C_{11}=390 GPa, C_{33}=398 GPa, and C_{44}=105 GPa. Our results show that the difference in the calculated branch-averaged group velocity between the two sets is relatively small. The small difference is probably due to the relatively close values between C_{11} and C_{33}. Thus, in subsequent simulations, we use set I for all calculations. However, studies on coated GaN nanowires have suggested that for certain values of the wave vector such difference can be considerable.[28]

Thermal conductivity, κ, of GaN nanowires at room temperature as a function of wire diameter ranging from 20 to 140 nm is shown in Fig. 4(a). The rate of change in κ with respect to diameter is also shown in Fig. 4(b). The circles
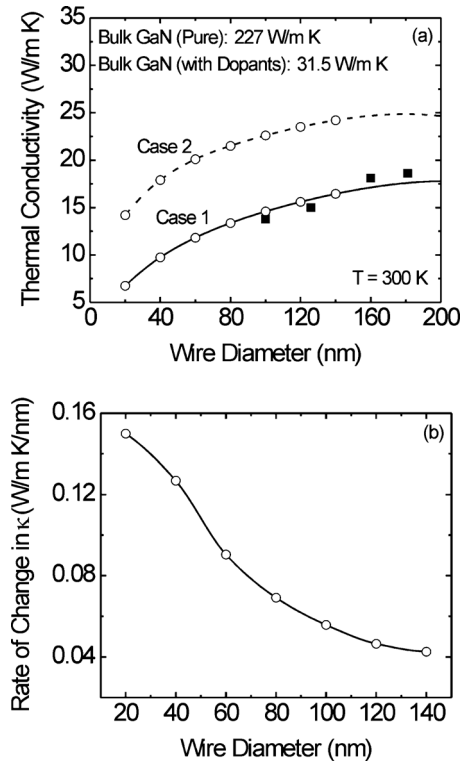
FIG. 4. (a) Thermal conductivity of GaN nanowires at room temperature ($T=300$ K) as a function of wire diameter; (b) rate of change in thermal conductivity, κ, with respect to wire diameter. Circles indicate calculated data and the dashed and solid curves are results after interpolation. Square symbols represent experimental data extracted from Ref. 10. The simulation results are obtained in two cases: in case 1 (solid), we consider the change in the nonequilibrium phonon distribution due to diffuse scattering at the wire surfaces; whereas in case 2 (dashed), we do not. Both cases have included phonon confinement, boundary scattering, and scattering on impurities and electrons. It can be seen that the results obtained in case 1 are in excellent agreement with the experimental data. Calculated thermal conductivity of pure and doped bulk GaN is also shown. Material parameters used include $n_e=2.3\times10^{19}$ cm^{-3} and Si and O impurity concentrations at 0.13 and 0.01 at. %, respectively.

indicate the calculated data and the dashed and solid lines are results after interpolation. Calculations are performed in two cases: in case 1, we consider the change in the nonequilibrium phonon distribution due to diffuse scattering at the wire surfaces; whereas in case 2, we do not. Both cases have included phonon confinement, boundary scattering, and scattering on impurities and electrons. Experimental data extracted from Ref. 10 are given in square symbols. For comparison, thermal conductivity of bulk GaN with and without dopants is also calculated. Our results show that for a pure bulk GaN crystal, $\kappa_{\text{bulk}}=227$ W/m K, which agrees very well with the experimental data[7] ($\kappa=225$ W/m K) on thick GaN films with a low dislocation density ($\sim10^6$ cm^{-2}) and dopant concentration ($\sim10^{16}$ cm^{-3}). At a dopant concentration of $n_e=2.3\times10^{19}$ cm^{-3}, it is shown that the thermal conductivity in the bulk is significantly reduced to $\kappa_{\text{bulk}}=31.5$ W/m K. Florescu *et al.*[6] have reported the measurements of thermal conductivity of GaN films (5–14 μm) fabricated by HVPE as a function of the carrier concentration n_e. They found that thermal conductivity decreased with $\log(n_e)$: about a factor of 2 decrease in κ for every decade increase in n_e. According to the above experimental observa-

tion, at a dopant concentration of $\sim10^{19}$ cm^{-3}, the thermal conductivity in the bulk is expected to be $\kappa_{\text{bulk}} \approx 28.1$ W/m K, which agrees well with our theoretical calculation. The large decrease in κ_{bulk} is mostly due to phonon point-defect scattering on dopants (impurities).[8]

Next, we show our calculations of the thermal conductivity of GaN nanowires and compare our results with experimental data. The dopant concentration used in the simulations is $n_e=2.3\times10^{19}$ cm^{-3}.[10] Results are shown in Fig. 4(a) with the solid line for case 1 and the dashed line for case 2. First, it can be seen that in both cases the thermal conductivity of the nanowires is considerably reduced from that of the bulk. For example, at $D=20$ nm, $\kappa_{\text{wire}}=6.74$ W/m K in case 1 and 14.2 W/m K in case 2, which correspond to 21% and 45% of the bulk value ($\kappa_{\text{bulk}}=31.5$ W/m K). Increased boundary scattering and phonon confinement play an important role in reducing the thermal conductivity of the nanowires. Boundary scattering reduces the phonon mean free path and increases the thermal resistance. Phonon confinement leads to flattening of the phonon dispersion and decreased phonon group velocity (see Figs. 1 and 2). Due to the $1/V^3$-dependence of the point-defect scattering, a decrease in the phonon group velocity leads to an increase in the scattering rate, $1/\tau_P$, and a corresponding decrease in the thermal conductivity. On the other hand, boundary scattering depends linearly on the phonon velocity, V. Thus, a decrease in V also leads to a decrease in $1/\tau_B$ and a reduced thermal resistance. Therefore, the effects of boundary scattering and phonon confinement should not be treated separately, but rather should be considered jointly in the calculation of thermal conductivity. Second, we compare the results obtained in case 1 and case 2. Figure 4(a) shows that in the range of $D =20-140$ nm, $\kappa_{\text{wire}}=6.74-16.4$ W/m K in case 1 and $\kappa_{\text{wire}}=14.2-24.2$ W/m K in case 2. Thus, our calculations have shown that the change in the nonequilibrium phonon distribution due to diffuse boundary scattering leads to an additional reduction in the thermal conductivity of the nanowires. We now compare both results with recent experimental data on GaN nanowires grown by thermal CVD.[10] For a diameter range of 97–181 nm, the measured thermal conductivity of the nanowires was reported to be in the range of 13–19 W/m K at 300 K. Our calculations in case 1 show that for a comparable diameter range of $D=100-180$ nm, $\kappa_{\text{wire}}=14.6-18.0$ W/m K, which are in excellent agreement with the reported experimental data. The results obtained in case 2, however, are $\kappa_{\text{wire}}=22.6-24.9$ W/m K, which are overestimated compared to the experimental data. Thus, as shown in case 1, the change in the nonequilibrium phonon distribution due to diffuse boundary scattering is an important factor that has to be considered in the calculation of thermal conductivity. Finally, we show the dependence of thermal conductivity on wire diameter by calculating the rate of change in κ with respect to D. Figure 4(b) shows that the thermal conductivity of a nanowire increases with wire diameter. However, the rate of such increase gradually slows down, indicating a smaller diameter dependence of the thermal conductivity for larger values of D. For example, as shown in Fig. 4(b), at $D=20$ nm, the average rate of increase in κ with respect to D is ~0.15 W/m K/nm; whereas at

$D=140$ nm, such rate has dropped to $\sim$0.043 W/m K/nm. Our results are consistent with the experimentally observed weak diameter dependence of the thermal conductivity for D in the range of 97–181 nm.[10] The weaker diameter dependence of κ at larger D values can be explained by the decreased boundary scattering rate and thus the less influence of boundary scattering on the thermal resistance.

IV. CONCLUSIONS

We have calculated the thermal conductivity κ of free-standing GaN nanowires with diameters ranging from 20 to 140 nm. The calculations are material specific and performed with an impurity profile and dopant concentration characteristic of GaN nanowires grown by thermal CVD. Our calculations show that the nanowires exhibit very low thermal conductivity, ranging from 6.74 W/m K (for $D=20$ nm) to 16.4 W/m K (for $D=140$ nm). The obtained results are in excellent agreement with the experimental data on thermal CVD-grown GaN nanowires. We have further demonstrated that the very low value of κ is not only due to point-defect scattering, boundary scattering, and phonon confinement, but also due to the change in the nonequilibrium phonon distribution as a result of diffuse scattering at the wire surfaces. The latter leads to an additional reduction in κ and has to be considered in the simulation of thermal conductivity of nanowires. Our conclusion is different from a previous study which attributed the very low κ value to the unusually large mass-difference scattering in the samples. We have also verified the experimentally observed weak diameter dependence of κ for large diameter values. Our results show that at $D=140$ nm, the rate of change in κ is $\sim$0.043 W/m K/nm. The obtained results are important for the high-power/high-temperature device applications based on GaN nanowires.

ACKNOWLEDGMENTS

[1] H.-J. Choi, J. C. Johnson, R. He, S.-K. Lee, F. Kim, P. Pauzauskie, J. Goldberger, R. J. Saykally, and P. Yang, J. Phys. Chem. B **107**, 8721 (2003).

[2] T. Westover, R. Jones, J. Y. Huang, G. Wang, E. Lai, and A. A. Talin, Nano Lett. **9**, 257 (2009).

[3] F. Qian, S. Gradečak, Y. Li, C.-Y. Wen, and C. M. Lieber, Nano Lett. **5**, 2287 (2005).

[4] Y. Huang, X. Duan, and C. M. Lieber, Small **1**, 142 (2005).

[5] A. Witek, Diamond Relat. Mater. **7**, 962 (1998).

[6] D. I. Florescu, V. M. Asnin, F. H. Pollak, R. J. Molnar, and C. E. C. Wood, J. Appl. Phys. **88**, 3295 (2000).

[7] W. Liu, A. A. Balandin, C. Lee, and H.-Y. Lee, Phys. Status Solidi A **202**, R135 (2005).

[8] J. Zou, D. Kotchetkov, A. A. Balandin, D. I. Florescu, and F. H. Pollak, J. Appl. Phys. **92**, 2534 (2002).

[9] Z. Wang, X. Zu, F. Gao, W. J. Weber, and J.-P. Crocombette, Appl. Phys. Lett. **90**, 161923 (2007).

[10] C. Guthy, C.-Y. Nam, and J. E. Fischer, J. Appl. Phys. **103**, 064319 (2008).

[11] C. M. Bhandari and D. M. Rowe, *Thermal Conduction in Semiconductors* (Wiley, New York, 1988).

[12] A. Balandin and K. L. Wang, Phys. Rev. B **58**, 1544 (1998).

[13] A. Khitun, A. Balandin, and K. L. Wang, Superlattices Microstruct. **26**, 181 (1999).

[14] S. G. Walkauskas, D. A. Broido, K. Kempa, and T. L. Reinecke, J. Appl. Phys. **85**, 2579 (1999).

[15] J. Zou and A. Balandin, J. Appl. Phys. **89**, 2932 (2001).

[16] J. M. Ziman, *Electrons and Phonons* (Clarendon, Oxford, 1960).

[17] D. G. Cahill, W. K. Ford, K. E. Goodson, G. G. Mahan, A. Majumdar, H. J. Maris, R. Merlin, and S. R. Phillpot, J. Appl. Phys. **93**, 793 (2003).

[18] B. A. Auld, *Acoustic Fields and Waves in Solids* (Wiley, New York, 1973).

[19] S. Yu, K. W. Kim, M. A. Stroscio, and G. J. Iafrate, Phys. Rev. B **51**, 4695 (1995).

[20] T. Deguchi, D. Ichiryu, K. Toshikawa, K. Sekiguchi, T. Sota, R. Matsuo, T. Azuhata, M. Yamaguchi, T. Yagi, S. Chichibu, and S. Nakamura, J. Appl. Phys. **86**, 1860 (1999).

[21] J. Zou, X. Lange, and C. Richardson, J. Appl. Phys. **100**, 104309 (2006).

[22] D. Tham, C.-Y. Nam, and J. E. Fischer, Adv. Funct. Mater. **16**, 1197 (2006).

[23] P. G. Klemens, in *Chemistry and Physics of Nanostructures and Related Non-Equilibrium Materials*, edited by E. Ma, B. Fultz, R. Shall, J. Morral, and P. Nash (Minerals, Metals, and Materials Society, Warrendale, PA, 1997), p. 97.

[24] P. G. Klemens, in *Solid State Physics*, edited by F. Seitz and D. Turnbull (Academic, New York, 1958), Vol. 7.

[25] P. G. Klemens, Proc. Phys. Soc., London, Sect. A **68**, 1113 (1955).

[26] J. Yang, G. P. Meisner, and L. Chen, Appl. Phys. Lett. **85**, 1140 (2004).

[27] J. E. Parrott, Rev. Int. Hautes Temp. Refract. **16**, 393 (1979).

[28] E. P. Pokatilov, D. L. Nika, and A. A. Balandin, Superlattices Microstruct. **38**, 168 (2005).